Self-Assembly and Electrochemical Oxidation of Polyamidoamine–Carbazole Dendron Surfmer Complexes: Nanoring Formation

Chatthai Kaewtong,[†,‡] Guoqian Jiang,[†] Mary Jane Felipe,[†] Buncha Pulpoka,[‡,*] and Rigoberto Advincula[†,*]

[†]Department of Chemistry and Department of Chemical and Biomolecular Engineering, University of Houston, Houston, Texas 77204-5003, and [‡]Supramolecular Chemistry Research Unit and Organic Synthesis Research Unit, Department of Chemistry, Faculty of Science, Chulalongkorn University, Bangkok 10330, Thailand

ABSTRACT We report a detailed and quantitative study on the supramolecular complexation of amine-functionalized polyamidoamine (PAMAM) dendrimer G_4-NH_2 with carboxylic acid terminal dendrons containing peripheral electroactive carbazole groups of different generations (G_0COOH, G_1COOH, and G_2COOH). While the focus is on a detailed understanding and mechanism of complex formation, subsequent electrochemical oxidation of the dendron surfmers resulted in the formation of *nanoring* structures electrodeposited on the conducting substrate. Complexation was confirmed by NMR, UV–vis, and IR measurements. Critical micelle concentration (CMC), atomic force microscopy (AFM), and X-ray photoelectron spectroscopy (XPS) studies revealed that the ringlike structures were formed during the equilibrium–decomplexation stage and that the electrochemical process did not destroy the complex but rather stabilized it. The different generations of the dendrons provided various structures and complex formation efficacy. This type of template polymerization combined with electrochemically anodic oxidation has not been previously reported.

KEYWORDS: carbazole dendron · PAMAM · complexation · template polymerization · nanoring

Supramolecular nanostructures derived from self-organizing molecules and macromolecules are of high interest for achieving new functions and properties in the fields of material science and chemical biology.[1–6] Dendrimeric self-assembly, especially in the case of polyamidoamine (PAMAM) dendrimers, has attracted increasing attention in recent years because of their unique structures, interesting properties, and ready availability.[7–16] Their potential applications in medicine, catalysis, gene therapy, and nanoreactor systems have been explored in the past decade or so.[17–19] These dendrimers are composed of a central core (ethylenediamine, in this study) with amidoamine branching units that extend outward in a symmetric fashion and consist of *n* generations (layers). Polyamidoamine is a monodispersed, highly branched macromolecule with primary amine functional groups on the surface and amido units at the branch points in the interior including internal tertiary amines. Recently, a number of studies have focused on the interaction and aggregation behavior between PAMAM dendrimers and surfactants in aqueous solution such as SDS,[20–23] poly(ethylene glycol),[24] and dodecanoic acid.[25] However, up to now, there has been no attempt to use PAMAM–surfactant complexes as templates for directed polymerization. Template polymerization is a useful method to obtain multicomponent materials.[26–28] A polymer can be used as a template to associate monomers by noncovalent interactions such as hydrogen bonding, electrostatic forces, dipole forces, and other interactions, followed by polymerization of the monomers on the contours of the template.[29] Thus, a template acts as a structure-directing agent guiding the topology of the polymerization process. In direct templating, a change of dimensions or phase transitions occurs, and the templated material becomes a 1:1 copy of a template. Template polymerization of polyelectrolyte–surfactant monomer (surfmer) complexes is a primary example and has been previously reviewed.[30–34] They were successfully demonstrated in the polymerization of a variety of lipid assemblies with preservation of the mesostructures. However, γ-irradiation has been shown to degrade the monomer in the initiation step of a polymerization reaction within smectic liquid–crystalline layers.[35] Recently, Faul et al.[30,31] have been able to preserve the lamellar phase structure of polyelectrolyte–surfmer surfactant (di(undeccenyl)phosphate and α-ω-diene) complexes through a dithiol polyaddition strategy. The outer shell of a nanosized

*Address correspondence to radvincula@uh.edu, pbuncha@gmail.com.

Received for review February 16, 2008 and accepted July 05, 2008.

Published online July 25, 2008.
10.1021/nn800098j CCC: $40.75

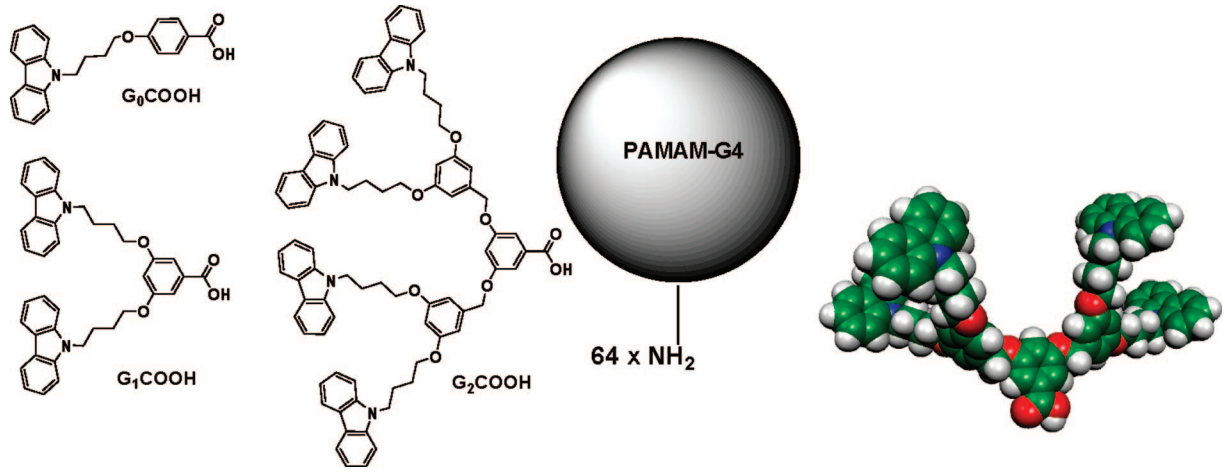

Figure 1. PAMAM dendrimer G_4-NH_2 with carboxylic acid terminal dendrons containing peripheral electroactive carbazole groups of different generations (G_0COOH, G_1COOH, and G_2COOH). The optimized structures of G_2COOH built from the Gaussian 98 B3LYP/STO-3G output file using the "Molekel" software are also shown.

macromolecule can be intracross-linked in a controlled manner through metathesis polymerization techniques. Zimmerman et al. previously reported the "self-assembly" of homoallyl dendrons into a cored dendrimer, and reversibility of the ring-closing metathesis mediated cross-linking of the dendrimers.[36,37]

Electroactive groups such as pyrrole[38,39] and thiophene[40,41] containing surfactants have the potential for producing new hybrid and electro-optical materials. Because of the electroactive moieties, they are not only polymerizable but also potentially electrically conductive when polymerized. Nanowire structures of polypyrrole, polyaniline, and thiophene have been realized which could serve as new conducting fibers.[42–44] On the other hand, carbazole polymers have been of recent interest due to their interesting electrochemical homopolymerization and copolymerization behavior.[45] They exhibit interesting electrochromic properties as well.[46] The ability of polycarbazole to form two distinct oxidation states further leads to multichromic effects.[47–49] Furthermore, polycarbazole is well-known as a hole transport material.[50] Morin and Leclerc reported the synthesis of a series of 2,7-carbazole-based conjugated polymers and their unique electrochemical and optical properties.[51–54] A recent review highlighted the interesting electrochemical and optical properties of oligomeric and polymeric carbazole-based materials as well as their tunable physicochemical properties using different synthetic strategies and substitution patterns.[55]

In this paper, we report a detailed and quantitative study on the supramolecular complexation of amine-functionalized PAMAM dendrimer G_4-NH_2 with carboxylic acid focal point functionalized dendrons containing terminal electroactive carbazole groups of different generations (G_0COOH, G_1COOH, and G_2COOH) (Figure 1). The focus is on a detailed understanding and mechanism of complex formation and subsequent electropolymerization properties with the different generations of the dendron surfmers. In the process, we observed the formation of interesting *nanoring* structures that preceded the electropolymerization process. The rest of the work involved understanding the nature of this nanostructure formation. To the best of our knowledge, there has been no report in which template polymerization was applied with a dendrimer−surfmer complex via electropolymerization.

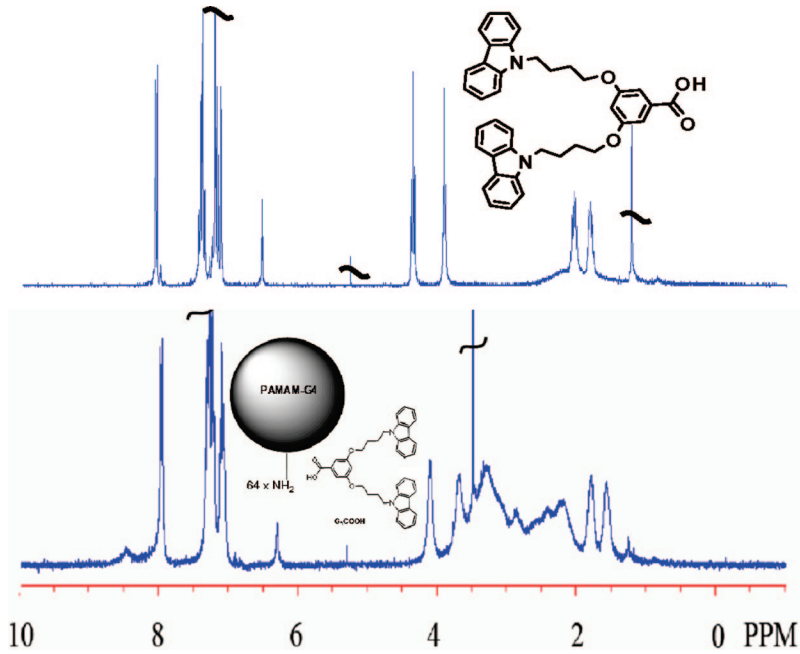

Figure 2. ^{1}H NMR spectra (300 MHz, 298 K) in $CDCl_3$ of 2 mM solutions (based on the concentration of PAMAM) of (a) G_1COOH and (b) complex of PAMAM−G_1COOH.

RESULTS AND DISCUSSION

The amine-terminated, ethylene diamine core, G_4-poly(amidoamine) dendrimer (G_4[EDA] PAMAM-NH_2), has 64 primary amines on the

surface. The surfmer anionic carbazole (CBz) dendrons (G_0COOH, G_1COOH, and G_2COOH) were prepared according to modified procedures recently reported by our group (details in the Supporting Information or SI).[56] The zero-, first-, and second-generation anionic dendronized macromolecules were selected to form ionic supramolecular complexes. The entire set of complexes between the dendron surfactants and PAMAM was carried out with stoichiometric ratios of the carboxylic acid group on the dendrons and the primary amines on the surface. A suspension of CBz dendrons (6.4 μmol) was prepared in MeOH (0.82 mL). It was then stirred at 25 °C, after which the G_4-PAMAM solution (0.1 μmol in 0.18 mL of MeOH) was added dropwise. After 24 h, a clear solution was obtained. The formation of the spherical assemblies of the G_0COOH and G_1COOH with G_4-PAMAM was then monitored by ^{1}H NMR spectroscopy in $CDCl_3$. In the absence of PAMAM, the ^{1}H NMR spectra chemical shifts of G_1COOH were very clear, sharp, and assignable as shown in Figure 2a as well as G_0COOH in Figure S1. When PAMAM was titrated into the G_0COOH and G_1COOH solutions, all signals shifted upfield, and the resonance for the spectra broadened after stirring for 24 h, suggesting the translational movement and compact aggregation of the dendrons to the PAMAM surface.[57–59] The chemical shifts of the PAMAM dendrimer were also detected at $\delta = 2.0-3.5$ ppm. However, despite several attempts, complexation of G_2COOH with PAMAM was not observed, which may be the result of steric effects and lack of solubility in the G_2COOH. The UV−vis spectra before and after the complexation of G_0COOH and G_1COOH with PAMAM are shown in Figure 3a. Absorption peaks are observed at 265, 295, 330, and 345 nm, which are typically assigned to the $\pi-\pi^*$ and $n-\pi^*$ transitions of carbazole.[60–63] In the case of the G_1COOH, it can be dissolved in more polar (MeOH) as well as less polar ($CHCl_3$) solvents. In MeOH, the peaks are ~5 nm blue-shifted when compared with those of $CHCl_3$ solution. On the other hand, G_0COOH could be dissolved very well in $CHCl_3$ but was insoluble in MeOH. This eventually influenced the G_0COOH−PAMAM to have stronger aggregation characteristics as compared to the G_1COOH−PAMAM in MeOH. In all cases, hypsochromic shifts were observed upon addition of PAMAM into the solutions of G_1COOH. As shown in Figure 3b and SI Figure S3, fluorescence studies revealed a decrease in fluorescence emission up to 70% upon addition of PAMAM. The quenching phenomenon is most likely attributed to the conformational change[64–66] due to aggregation of the carbazole groups as they stacked on the periphery of PAMAM. It should be noted that the equilibrium between complexation and decomplexation has an influence on the percentage of quenching. Accordingly, up to 30% of the quenching with G_0COOH−PAMAM is attributed to the formation of complex species, consistent with their aggregation properties.

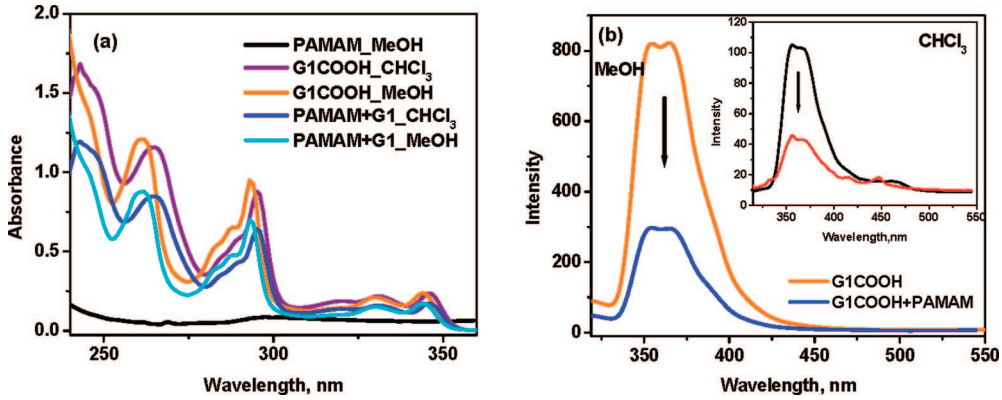

Figure 3. (a) UV−vis absorption spectrum of G_1COOH solutions in MeOH and $CHCl_3$ before and after complexation with PAMAM. (b) Fluorescence emission spectrum of G_1COOH before and after complexation with PAMAM, $\lambda_{ex} = 293$ nm, $\lambda_{em} = 360$ nm.

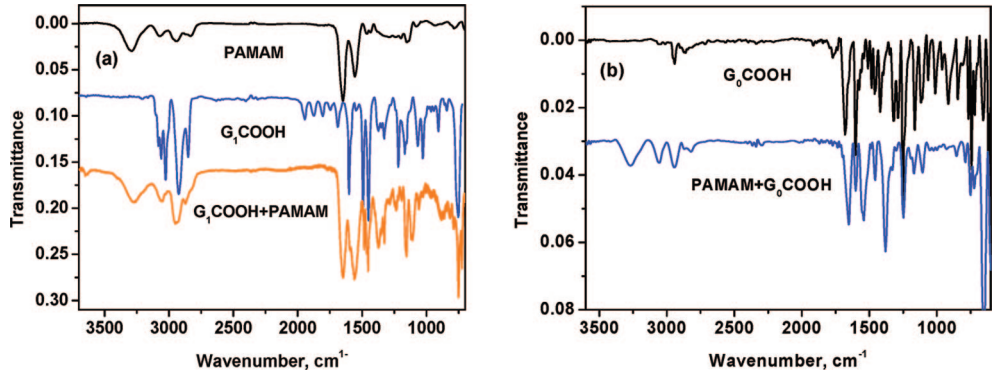

Figure 4. FTIR spectra of (a) PAMAM, G_1COOH, and the G_1COOH−PAMAM complex and (b) G_0COOH and the G_0COOH−PAMAM complex. Resolution is at 4 cm^{-1} for each spectrum.

To further test whether the PAMAM actually formed complexes with G_0COOH and G_1COOH, FT-IR spectra were recorded after 24 h addition of PAMAM solution to G_0COOH and G_1COOH (at 25 °C, clear solutions were obtained). Shown in Figure 4 a are the IR spectra of PAMAM, G_1COOH, and the G_1COOH + PAMAM complex (KBr). The carboxylic acid vibrations for G_1COOH were found to be at 1690 cm^{-1} (C═O stretch, dimer) and at 1373 cm^{-1} (C−O stretch, dimer) and changed to a broad diffuse band between 1500 and 1760 cm^{-1} in the spectrum of the G_1COOH−PAMAM complex result-

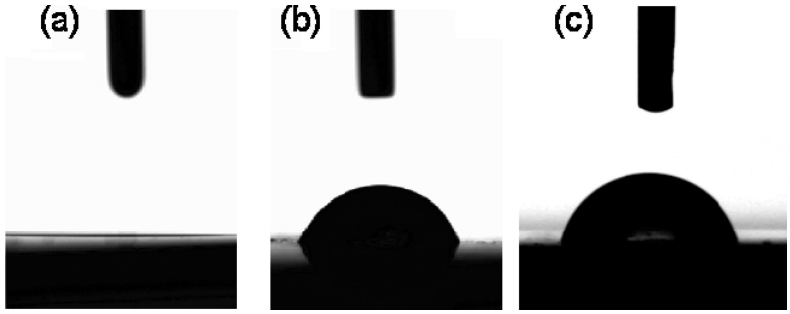

Figure 5. WCA measurement for: (a) PAMAM (0°); (b) complex PAMAM−G_1COOH (55.7°); and (c) complex PAMAM−G_0COOH (80.3°).

ing from the ionic ammonium carboxylate structures. The same results were observed on the studies of PAMAM−G_0COOH, where the carboxylic dimer peaks at 1758 and 1303 cm^{-1} changed to broad diffuse bands of ionic carboxylate structures between 1500 and 1600 cm^{-1}. According to these results, it can be concluded that 1:1 stoichiometric complexes were formed similar to previously reported fluorinated[67] and nonfluorinated[68] polyethyleneimine complexes.

Contact angle measurements were also carried out to investigate the complexation. In this case, the complexation should reduce the hydrophilicity of the PAMAM and the dendrons (Figure 5). The dilute solutions of the PAMAM and the complexes were spin-coated on a precleaned and plasma treated Si-wafer flat substrate. The films prepared from the complexes of G_0COOH and G_1COOH and the PAMAM solutions resulted in a change of the static water contact angle (WCA) (0° to 55.7°, G_1COOH, and 0° to 80.3°, G_0COOH). This confirmed the complexation of PAMAM with dendrons based on a change in the hydrophilic−lipophilic balance (HLB) compared to the completely wetted PAMAM−Si-wafer substrate, with a WCA of 0°. The large increase in WCA is due to the hydrophobicity of the carbazole groups forming the outer shell of the dendrimers. From these results, it can also be inferred that the G_0COOH is strongly associated on the peripheral of the dendrimer and is fully complexed compared to G_1COOH, as confirmed by the larger WCA increase on the former.

The formation of the individual PAMAM−G_1COOH dendrimer−surfmer complexes was directly observed by atomic force microscopy (AFM) as shown in Figure 6 and SI Figure S4. Very dilute solutions of 1 μM of the PAMAM−G_1COOH complexes in MeOH and $CHCl_3$ were spin-casted onto mica substrates. Isolated nanoparticles of the dendrimer complexes were observed on the surface when 10^{-6} M concentration was used. The particle diameter of PAMAM is 4.0 ± 0.5 nm, and PAMAM−G_1COOH complexes in MeOH and $CHCl_3$ are determined to be 7.0 ± 0.5 and 16.5 ± 1.0 nm, respectively. The difference in the complex's size was verified by molecular modeling (Gaussian 98 with B3LYP/STO-3G basic set) (Figure 7). From optimization of the structures, two different conformers were found to have the same minimum energy. The sizable increase with complexation is dependent on the polarity of solvent. It can be noted that conformer **a** will be present in MeOH to avoid the polar solvent and conformer **b** will be present in $CHCl_3$, a more nonpolar solvent. Moreover, by decreasing the generation of dendron to G_0COOH, a smaller increase of the diameter with 4.3 ± 0.5 nm was found, as demonstrated in SI Figure S4. It is clear that G_0COOH has a stronger aggregation after complexation.

Cyclic Voltammetry Studies. The studies on electrochemical oxidation of carbazole have been reported for some time now. Ambrose et al. investigated the mechanism of anodic oxidation of carbazole and its N-substituted derivatives.[69,70] During the anodic oxidation process, coupling of two carbazolium radical cations at 3 and 3′ positions seems to be the predominant pathway, especially in the case of N-substituted derivatives. The highly stable N-substituted 3,3′-dicarbazyl prohibited the formation of more extended conjugation units, e.g., oligo- or polycarbazole. On the other hand, Schreck et al. reported the electrodeposition of a longer conjugation of "polycarbazole" (most likely tetramer) film under protic media.[71,72] More recently, electrochemical analysis also suggested anodic oxidation only led to 3,3′-dicarbazyl formation in the case of 2,7-carbazole-based conjugated polymers.[54] Herein, we aimed to employ cyclic voltammetry to anodically oxidize and cross-link the carbazoles on the PAMAM periphery and understand the effect of CV conditions (monomer concentration, applied potential, etc.) on the eventual optical and morphological properties of the electrode-

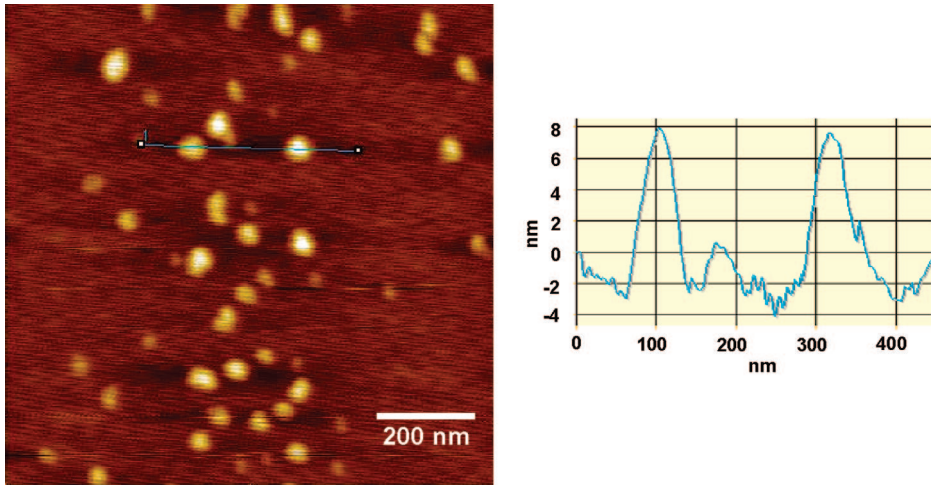

Figure 6. AFM image (1 × 1 μm) of the individual PAMAM−G_1COOH complexes on a mica substrate prepared from MeOH. The average diameter of the complexes was determined to be 7.0 ± 0.5 nm, and here the heights of the chosen particles were estimated to be ~10 nm from the step-depth analysis.

posited films. The precursor complexes (PAMAM−G_0COOH and PAMAM−G_1COOH) were electropolymerized and deposited on ITO substrates. The cyclic voltammetry (CV) curves are shown in Figure 8 and SI Figures S5 and S6. The potentials were cycled from 0 to 1.1, 1.3, and 1.5 V at a scan rate of 50 mV/s against Ag/AgCl reference electrode and platinum counter electrode. At a concentration of 10^{-6} M, no apparent redox peaks were observed on the anodic scan up to a potential of 1.1 V (Figure S5). As we can see from Figure 8a and b, when the potential window increased up to 1.3 and 1.5 V, the first oxidation peak was observed at 1.1 V resulting from the formation of carbazolium radical cations which underwent rapid coupling to 3,3′-dicarbazyls. Starting from the second anodic scan, two new peaks at 0.85 and 1.27 V appeared, corresponding to the radical cation and bication species of the dimer units, respectively. These results were in good agreement with earlier reports.[60,69,70,73] However, at a concentration of 10^{-5} M, the shape of the redox peaks in Figure 8c and d was not as pronounced as those at the lower concentration. This might be due to the nature of greater aggregation of the complexes at the higher concentration. In particular, as shown in Figure 8d, the redox peaks became much broader, indicating a more heterogeneous electron transfer process. This heterogeneous electron transfer is also likely a consequence of thicker films deposited during each CV cycle and can be confirmed by the higher intensity of the absorption peaks (following section). A small difference of the oxidation onsets was recorded in the anodic scans as shown in Figure 8 and Figure S6 and as summarized in Table S1. However, shape and peak positions are obviously unique for different concentrations and potential windows of the dendron complexes. From Table S1, it is obvious that PAMAM−G_1COOH shows a higher $\Delta E(E_{pa} - E_{pc})$ value than that of PAMAM−G_0COOH which indicates a more heterogeneous and slow electron-transfer rate for these complexes.[56]

Spectroelectrochemical Characterization. The electrodeposited films were further characterized by electrochemical UV−vis spectroscopy. The extent of the

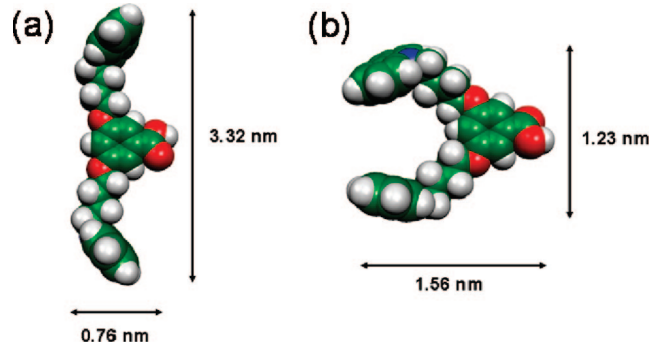

Figure 7. Optimized structures of G_1COOH built from the Gaussian 98 B3LYP/STO-3G output file using the "Molekel" software.

increasing π orbital overlap between neighboring repeating units on conjugated molecules can directly affect the observed energy of the π−π* transition which appears as the absorption maxima in the electronic spectra. The values of the absorption maxima for the different generations are closely linked to their degree of coupling. The extended appearance of the π−π* transition at 420−440 nm, which is attributed to the radical cations (polaronic band or doped state), is shown in Figure 9.[56,60−63,69] The peak between 600 and 1000 nm can be assigned to the π−π* transition of the dications (bipolaronic band or more highly doped state) originating from the formation of the conjugated 3,3′-dicarbazyl species complexing with hexafluorophosphate ions. From the spectra, the peaks

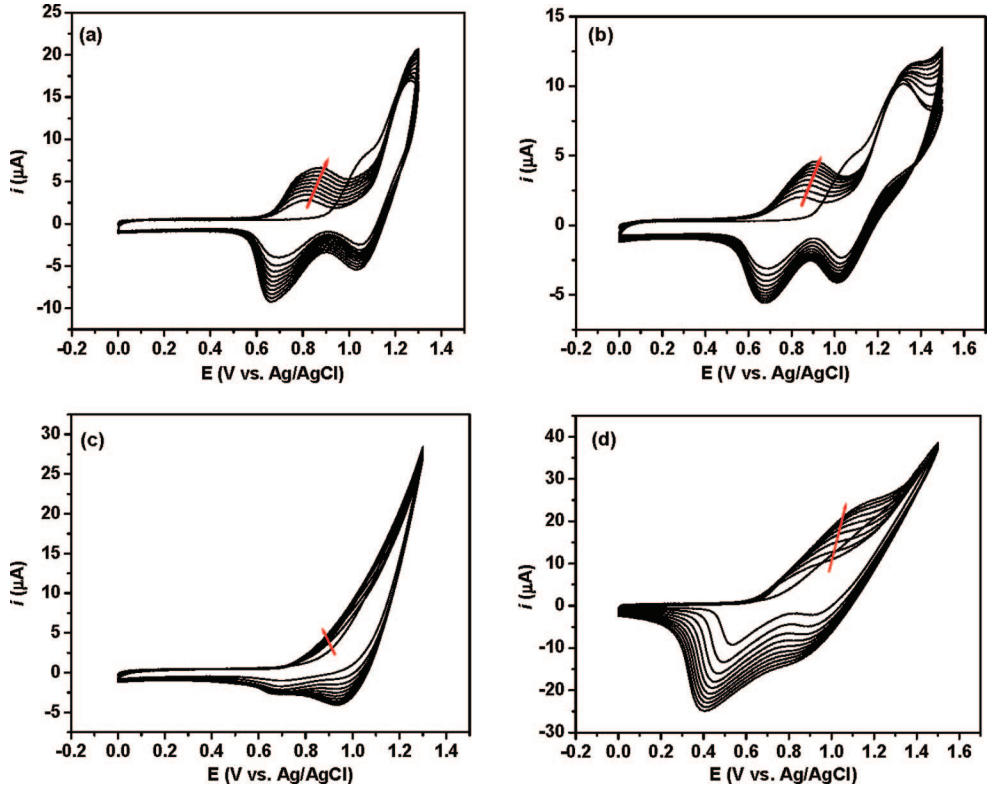

Figure 8. Cyclic voltammograms of the electrochemical polymerization of PAMAM−G_1COOH complexes at a scan rate of 50 mV/s, 10 cycles: (a) 10^{-6} M, potential window from 0 to 1.3 V, (b) 10^{-6} M, potential window from 0 to 1.5 V, (c) 10^{-5} M, potential window from 0 to 1.3 V, (d) 10^{-5} M, potential window from 0 to 1.5 V.

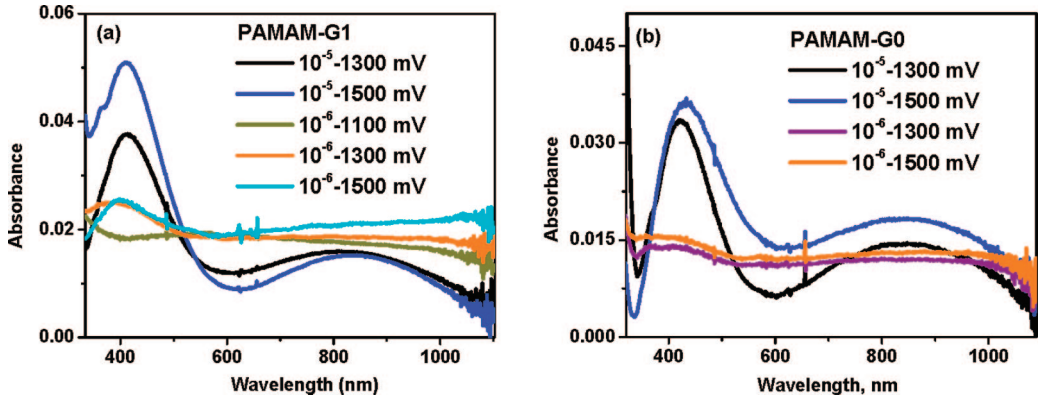

Figure 9. Absorption spectra analysis performed in 0.1 M $TBAPF_6/CHCl_3$ on ITO substrates in the presence of different concentrations and potential windows. (a) PAMAM−G_1COOH, (b) PAMAM−G_0COOH.

at high concentration and highly applied potential show extraordinary increases of the peak intensity at ~430 nm, and the appearance of the broad peak in the 600−1000 nm region confirms the highly conjugated nature of the materials deposited on the ITO substrates.

Morphological Studies. The morphology and molecular orientation of the dendron complexes after electrochemical deposition on ITO substrates have been studied using AFM measurements. In the case of PAMAM−G_1COOH at low concentration (10^{-6} M) and applied potential of 0−1.3 V, the AFM image in Figure 10a showed unique nanostructures (and also in SI Figure S7). These ringlike structures were ~75 nm in diameter and ~13 nm in height. Interestingly, this height is close to the full diameter of a PAMAM−G_1COOH nanoparticle diameter in $CHCl_3$. The diameter of the nanoring structure also closely resembles a donut shape particle that may likely contain a PAMAM core with the G_1COOH shell (Scheme 1). This kind of feature was observed repeatedly with solute evaporation[74] and is presumably related to the overall hydrophobic−hydrophilic balance property.[75,76] To investigate the mechanism that drives the morphological change from the micellar nanosphere (before electro-deposition) to ringlike (donut) nanostructures (after electrodeposition), two experiments were performed to determinate when the nanoring structures are formed as illustrated in Scheme 1.

The micellization phenomenon of G_1COOH was first investigated. If the critical micelle concentration (CMC) is equal to and/or less than the concentration of G_1COOH that was used to make PAMAM−G_1COOH complexes, the nanoring can be generated between the equilibrium of the G_1COOH micellization and the weak complexation equilibrium with the PAMAM. However, if the CMC is higher than the concentration of G_1COOH used, the equilibrium between weak and strong complexation with PAMAM should be preferred. We have studied the solubilization of the dye Nile Red as a function of the concentration of G_1COOH in order to determine the CMC.[77] Shown in Figure S8a is the UV−vis spectra before and after micelle formation, while Figure S8b represented the fluorescence spectra at λ_{ex} = 570 and λ_{em} = 655 nm of different solutions of G_1COOH. The dendron solution was stirred for 2 h in the presence of Nile Red and then filtered to remove unsolubilized dyes. The CMC of this system was found to be 70.0 μM. From the experiment, a 6.4 μM concentration of G_1COOH was used for dendron complexation, and a concentration of 1.0 μM was used for the CV. This means that the nanoring structures could have only formed at the equilibrium between the strong

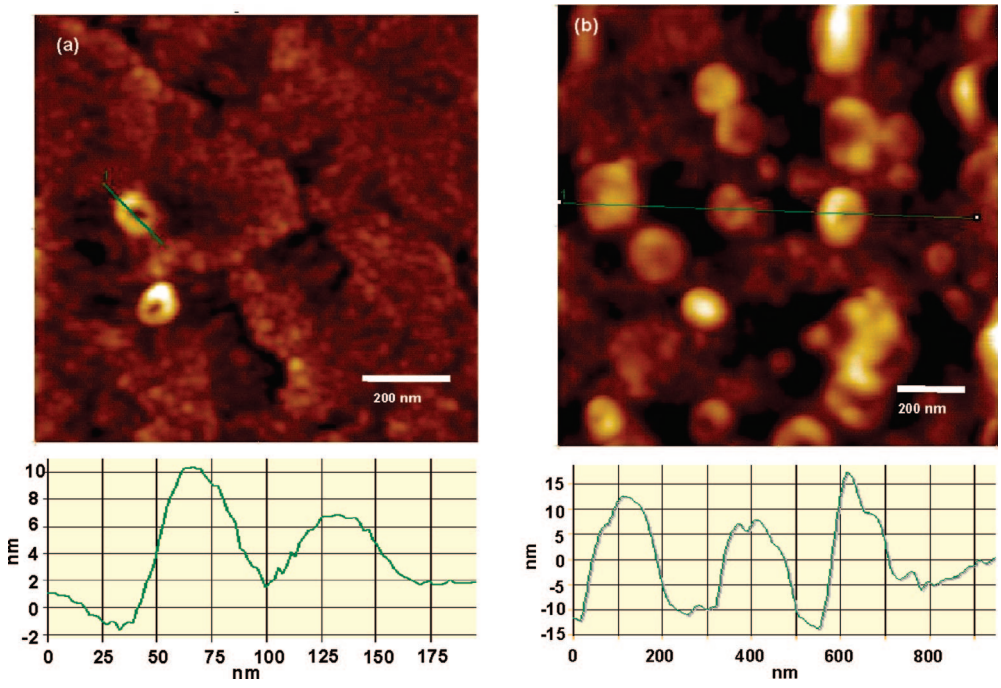

Figure 10. Tapping-mode AFM topography images of PAMAM−G_1COOH complexes after being electropolymerized on ITO at a scan rate of 50 mV/s, 10 cycles: (a) 10^{-6} M, potential window from 0.0 to 1.5 V, (b) 10^{-5} M, potential window from 0.0 to 1.3 V.

complexation and weak complexation stage as presented in Scheme 1 since there are not enough unimers to form free G_1COOH micelles based on these concentrations.

To test whether the nanoring structures could not have developed in the absence of PAMAM, we also studied the electrochemical oxidation of G_1COOH alone. The CV curves in Figure S9 exhibited similar oxidation and reduction peaks of the highly conjugated dicarbazyls. The linear current increase and ΔE change indicated that G_1COOH can also be effectively deposited on ITO with even greater efficiency than the PAMAM−G_1COOH. The in situ spectroelectrochemical studies also showed the typical $\pi-\pi^*$ transitions of the polaronic and bipolaronic bands of conjugated carbazoles. However, *no* ringlike nanostructures were observed on the morphology from the AFM images (Figure S10).

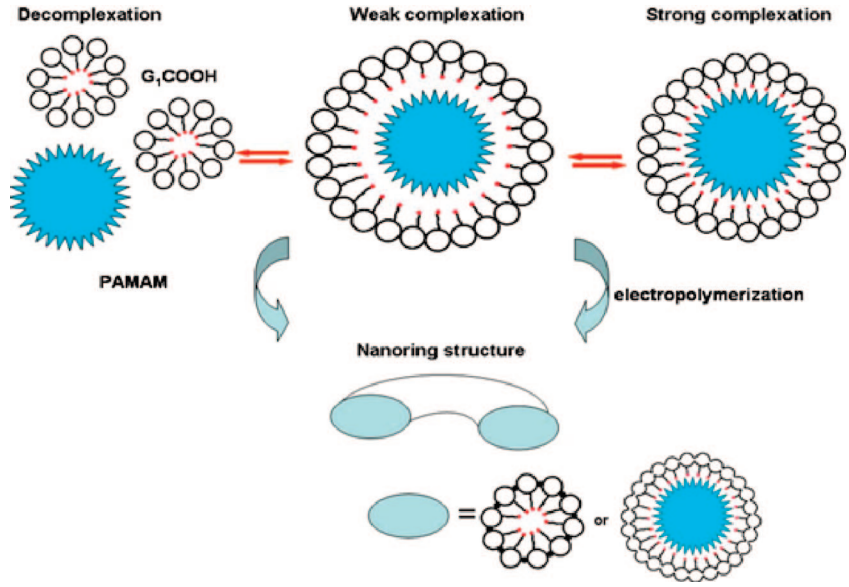

Scheme 1. Description of the formation of the nanoring structures between the equilibrium of decomplexation, weak complexation and strong complexation.

To further understand the components of the deposited film on the ITO, XPS spectroscopy was used to determine the composition of the deposited film based on the C/N ratio. Shown in Figure S11 is the high-resolution XPS spectrum of PAMAM−G_1COOH electrodeposited film on ITO for C and N atoms. In all quantitative analyses, the theoretical value is assumed on the basis of 100% electrografting. For the 10^{-6} M of PAMAM−G_1COOH electrodeposited with an applied potential up to 1.5 V, an experimental value of C/N = 7.95 was obtained which is higher than the theoretical value of PAMAM + G_1COOH at C/N = 7.07. This higher value indicates the incorporation of a slightly larger amount of the surfmer compared to the PAMAM core. Thus, during the electrochemical oxidation of the dendrimer complex, it is possible that the PAMAM was decomplexed into the solution subphase during the nanoring formation near the weak complexation equilibrium. Furthermore, since the surfmers are not likely to form micelles at the 10^{-6} M concentration used, the ring formation resulted in expulsion of the PAMAM and at the same time the electropolymerization of the dendron surfmer units. This explains the higher experimental C/N ratio observed from XPS and is supported by AFM, CMC, and even fluorescence data (carbazole aggregation). The rings then are formed largely due to the formation of a higher ordered core−shell ring (or donut) structure composed of a higher content of G_1COOH shell with PAMAM remaining as an interior template support during the electrochemical CV procedure.

Finally, to test the uniqueness of the dendron complexation phenomenon, we covalently bonded the G_1COOH to PAMAM to form a carbazole amide functionalized dendrimer (PC). The synthesis, purification, and characterization of this derivative are reported in the Supporting Information. The electopolymerization was carried out with the same parameters as with the

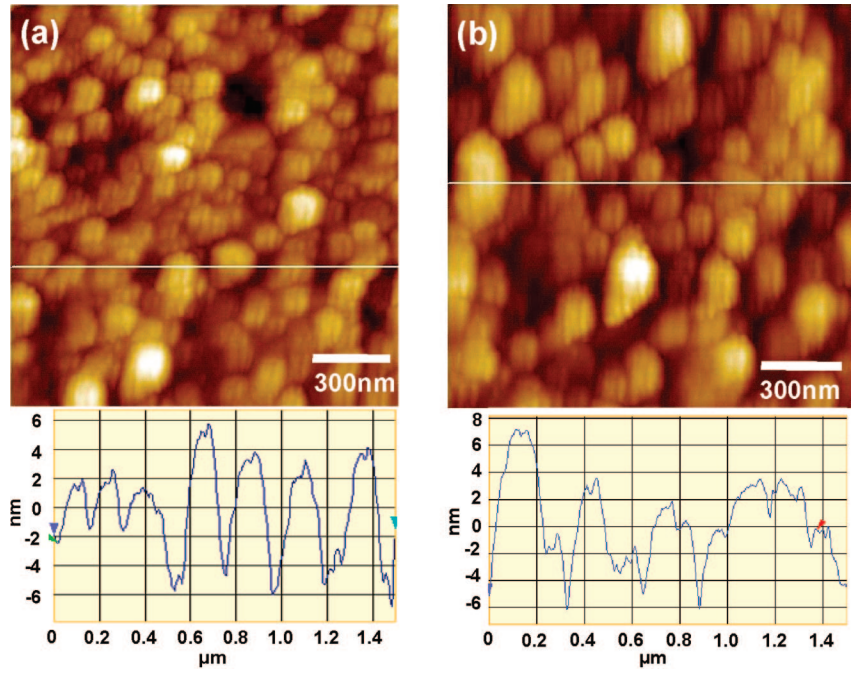

Figure 11. AFM topography images of 2-(3,5-bis(4-(9*H*-carbazol-9-yl)butoxy)phenyl)acetoyl-functionalized PAMAM (PC) after electropolymerization on ITO electrodes at a scan rate of 50 mV/s, 10 cycles: (a) 10^{-6} M, potential window from 0 to 1.3 V, (b) 10^{-5} M, potential window from 0 to1.3 V.

PAMAM−G_1COOH complexes. At the low potential application (1.3 V), a good trend of increasing oxidation potential onset was observed with the increase of cycles, but the CV curves shifted to higher anodic potential (E_{pa}) and the reduction peaks shifted to lower cathodic potential (E_{pc}) compared to the noncovalent PAMAM−dendron complexes as shown in Figure S7. Degradation was observed after applying the higher potential at 1.5 V which may come from the lack of availability of more mobile electroactive monomers. Moreover, the UV−vis spectra revealed the formation of similar polaron and bipolaron peaks as shown in Figure S13. From the morphology (Figure 11) as imaged by AFM, the PC film *did not* show nanoring formation at all but a rough and patchy surface that was macroscopically more nonuniform.

CONCLUSION

We have demonstrated the successful self-assembly and complexation between the dendrimer template (PAMAM G_4-NH_2) and dendron surfmers (G_0COOH, G_1COOH). The increasing steric hindrance of a dendron prevented complexation as in the case of G_2COOH. Hypochromic shifts in the UV−vis spectra and quenching of fluorescence indicated that G_1COOH was trapped around the dendrimer. Ammonium and carboxylate species were observed by FTIR. The isolated sphere size was observed on the mica substrates. The stronger complexation was observed in PAMAM−G_1COOH. The electrochemical oxidation of dendrimer complexes as thin films revealed unusual CV behavior depending upon the generation. PAMAM−G_1COOH showed a higher extent of anodic oxidation, while PAMAM−G_0COOH showed a higher degree of aggregation. More interestingly, nanoring structures were observed as the complex was deposited on ITO indicating a type of supramolecularly-based template electropolymerization of a dendrimer−surfmer complex. The CMC, AFM, and XPS revealed a ringlike or donut structure most likely composed of the PAMAM−core and dendron−carbazole shell. This was formed at the equilibrium of decomplexation and weak complexation. In principle, different generations of dendrons, different dendrimer topologies, and other electroactive surfmer moieties can result in a wider applicability of this method, for electro-optical, drug delivery, sensing, and other nanoscience and materials applications.

EXPERIMENTAL SECTION

Chemicals and Methods. All chemical reagents were purchased from Aldrich Chemical Co. unless otherwise stated. Solvents were acquired from Fisher. Tetrahydrofuran (THF) was distilled over sodium/benzophenone ketyl, and *N*,*N*-dimethylformamide (DMF) was purchased anhydrous or otherwise dried over Linde type 4-Å molecular sieves. Commercially available reagents were used without further purification unless noted otherwise. *N*-(4-Bromobutyl)-9*H*-carbazole was prepared according to literature procedures.[78]

Instrumentation. Nuclear magnetic resonance (NMR) spectra were recorded on a General Electric QE-300 spectrometer operating at 300 MHz for ^{1}H nuclei. UV−vis spectra were recorded using an Agilent 8453 spectrometer. UV−vis measurements of the films were carried out *in situ* on an ITO substrate. This was done using a Teflon flow cell manufactured with a modified ITO window and microscope slide window that was placed in the path of an HP-8453 diode array spectrometer. All FTIR measurements were performed using a Digilab FTS 7000 step scan spectrometer (Digilab, Randolph, MA) equipped with a liquid N_2-cooled MCT detector. KBr pellets were prepared by first mixing the sample solutions with KBr, removing solvents under vacuum, and then pressing the KBr using a 10 ton hydraulic press. The cyclic voltammetry (CV) experiments were carried out on a Princeton Applied Research Parstat 2263 with an ITO substrate as the working electrode coupled with a Pt plate as the counter electrode and a Ag/AgCl wire as the reference electrode. Atomic force microscopy (AFM) imaging was examined in ambient conditions with a PicoSPM II (PicoPlus, Molecular Imaging) in the tapping mode.

Preparation of the Complexes. The amine-terminated, ethylene diamine core, Generation 4 poly(amidoamine) dendrimer (G_4[EDA] PAMAM−NH_2, >99% purity) was purchased from Sigma-Aldrich and used without further purification. It has 64 primary amines on the surface and 180 tertiary amines at branch points within the core. The anionic carbazole (CBz) dendrons (G_0COOH, G_1COOH, and G_2COOH) were prepared according to the modified procedures that have been recently reported by our group, and the synthetic scheme and procedures were shown in the Supporting Information. Complex preparation: zero-, first-, and second-generation anionic dendronized macromolecules were selected to form ionic supramolecular complexes as illustrated in Scheme 1. The entire set of complexations between dendron surfactants and PAMAM was carried out with stoichiometric ratios of the carboxylic acid group on the dendrons and the primary amines on the surface. A suspension of CBz dendrons (6.4 μmol) was prepared in MeOH (0.82 mL). It was then stirred at 25 °C, after which PAMAM G4 solution (0.1 μmol in 0.18 mL of MeOH) was added dropwise. After 24 h, a clear solution was obtained. ^{1}H NMR spectroscopy was then used to monitor the complexation behavior of the CBz dendron and PAMAM every 2 h until complexation was found complete. All samples were kept under nitrogen to avoid any contamination by atmospheric carbon dioxide.

Acknowledgment. The authors acknowledge financial support from NSF-DMR (05-04435), NSF-DMR (06-02896), NSF-DMR (03-15565), Alliance for Nanohealth of Texas, and the Robert A. Welch Foundation (E-1551). B.P. and C.K. acknowledge support from the Thailand Research Fund (TRF) (RMU4880041) and the Royal Golden Jubilee Ph.D Program of TRF (PHD/0137/2546). C.K. also thanks Vithaya Ruangpornvisuti for suggestions and computational calculations on the dendron structures.

Supporting Information Available: Synthesis and characterization details, calculated structure of G_2COOH, UV−vis and fluorescence spectra of G_0COOH before and after complexation, AFM images of PAMAM and the complexes, summary of the CV redox peaks, CV curves of G_1COOH, PAMAM−$G_{0(1)}$ under different conditions and their corresponding AFM images, HR-XPS of the cross-linked polymer, CV curves of PC under different conditions, and spectroelectrochemical spectrum of PC electropolymerization. This material is available free of charge via the Internet at http://pubs.acs.org.

REFERENCES AND NOTES

1. Lehn, J. M. Supramolecular Chemistry and Self-Assembly Special Feature: Toward Complex Matter: Supramolecular

Chemistry and Self-Organization. *Proc. Natl. Acad. Sci. U.S.A.* **2002**, *99*, 4763–4768.
2. Lee, M.; Cho, B.-K.; Zin, W. C. Supramolecular Structures from Rod-Coil Block Copolymers. *Chem. Rev.* **2001**, *101*, 3869–3892.
3. Sarikaya, M.; Tamerler, C.; Jen, A. K.-Y.; Schulten, K.; Baneyx, F. Molecular Biomimetics: Nanotechnology through Biology. *Nat. Mater.* **2003**, *2*, 577–585.
4. Hoeben, F. J. M.; Jonkheijm, P.; Meijer, E. W.; Schenning, A. P. H. J. About Supramolecular Assemblies of π-Conjugated Systems. *Chem. Rev.* **2005**, *105*, 1491–1546.
5. Cornelissen, J. J. L. M.; Rowan, A. E.; Nolte, R. J. M.; Sommerdijk, N. A. J. M. Chiral Architectures from Macromolecular Building Blocks. *Chem. Rev.* **2001**, *101*, 4039–4070.
6. Tomalia, D. A. Birth of A New Macromolecular Architecture: Dendrimers as Quantized Building Blocks for Nanoscale Synthetic Polymer Chemistry. *Prog. Polym. Sci.* **2005**, *30*, 294–324.
7. Fischer, M.; Vögtle, F. Dendrimers: From Design to Application - A Progress Report. *Angew. Chem., Int. Ed.* **1999**, *38*, 884–905.
8. Frechet, J. M. J.; Tomalia, D. A. *Dendrimers and Other Dendritic Polymers*; Wiley Series in Polymer Science; Wiley: New York, 2001.
9. Newkome, G. R.; Moorefield, C. N.; Vögtle, F. *Dendrimers and Dendrons: Concepts, Synthesis, Applications*; Wiley-VCH: Weinheim, 2001.
10. Ossterom, G. E.; Reek, J. N. H.; Kamer, P. C. J.; van Leeuwen, P. W. N. M. Transition Metal Catalysis Using Functionalized Dendrimers. *Angew. Chem., Int. Ed.* **2001**, *40*, 1828–1849.
11. Astruc, D.; Chardac, F. Dendritic Catalysts and Dendrimers in Catalysis. *Chem. Rev.* **2001**, *101*, 2991–3024.
12. Grayson, S. M.; Frechet, J. M. J. Convergent Dendrons and Dendrimers: from Synthesis to Applications. *Chem. Rev.* **2001**, *101*, 3819–3868.
13. Stiriba, S. E.; Frey, H.; Haag, R. Dendritic Polymers in Biomedical Applications: from Potential to Clinical Use in Diagnostics and Therapy. *Angew. Chem., Int. Ed.* **2002**, *41*, 1329–1334.
14. Aulenta, F.; Hayes, W.; Rannard, S. Dendrimers: A New Class of Nanoscopic Containers and Delivery Devices. *Eur. Polym. J.* **2003**, *39*, 1741–1771.
15. Boas, U.; Heegaard, P. M. H. Dendrimers in Drug Research. *Chem. Soc. Rev.* **2004**, *33*, 43–63.
16. Svenson, S.; Tomalia, D. A. Dendrimers in Biomedical Applications-Reflections on the Field. *Adv. Drug Delivery Rev.* **2005**, *57*, 2106–2109.
17. Kim, Y. H.; Webster, O. W. Water Soluble Hyperbranched Polyphenylene: "A Unimolecular Micelle?". *J. Am. Chem. Soc.* **1990**, *112*, 4592–4593.
18. Newkome, G. R.; Moorefield, C. N.; Baker, G. R.; Johnson, A. L.; Behera, R. K. Alkane Cascade Polymers Possessing Micellar Topology: Micellanoic Acid Derivatives. *Angew. Chem., Int. Ed.* **1991**, *30*, 1176–1178.
19. Naylor, A. M.; Goddard, W. A., III; Kiefer, G. E.; Tomalia, D. A. Starburst Dendrimers. 5. Molecular Shape Control. *J. Am. Chem. Soc.* **1998**, *111*, 2339–2341.
20. Watkins, D. M.; Sayed-Sweet, Y.; Klimash, J. W.; Turro, N. J.; Tomalia, D. A. Dendrimers with Hydrophobic Cores and the Formation of Supramolecular Dendrimer-Surfactant Assemblies. *Langmuir* **1997**, *13*, 3136–3141.
21. Wang, C.; Wyn-Jones, E.; Sidhu, J.; Tam, K. C. Supramolecular Complex Induced by the Binding of Sodium Dodecyl Sulfate to PAMAM Dendrimers. *Langmuir* **2007**, *23*, 1635–1639.
22. Mizutani, H.; Torigoe, K.; Esumi, K. Physicochemical Properties of Quaternized Poly(amidoamine) Dendrimers with Alkyl Groups and of Their Mixtures with Sodium Dodecyl Sulfate. *J. Colloid Interface Sci.* **2002**, *248*, 493–498.
23. Sidhu, J.; Bloor, D. M.; Couderc-Azouani, S.; Penfold, J.; Holzwarth, J. F.; Wyn-Jones, E. Interactions of Poly(amidoamine) Dendrimers with the Surfactants SDS, DTAB, and $C_{12}EO_6$: An Equilibrium and Structural Study Using a SDS Selective Electrode, Isothermal Titration Calorimetry, and Small Angle Neutron Scattering. *Langmuir* **2004**, *20*, 9320–9328.
24. Chun, D.; Wudl, F; Nelson, A. Supramacromolecular Assembly Driven by Complementary Molecular Recognition. *Macromolecules* **2007**, *40*, 1782–1785.
25. Chechik, V.; Zhao, M.; Crooks, R. M. Self-Assembled Inverted Micelles Prepared from a Dendrimer Template: Phase Transfer of Encapsulated Guests. *J. Am. Chem. Soc.* **1999**, *121*, 4910–4911.
26. Polowinski, S. Template Polymerisation and Co-Polymerisation. *Prog. Polym. Sci.* **2002**, *27*, 537–577.
27. Szumilewicz, J. Molecular Recognition in Radical Template Polymerization. *Macromol. Symp.* **2000**, *161*, 183–190.
28. Polacco, G.; Cascone, M. G.; Petarca, L.; Maltinti, G.; Cristallini, C.; Barbani, N.; Lazzeri, L. Template Polymerization of Sodium Methacrylate onto Poly(allylamine) Hydrochloride. *Polym. Int.* **1996**, *41*, 443–448.
29. Serizawa, T.; Hamada, K.; Akashi, M. Polymerization within a Molecular-Scale Stereoregular Template. *Nature* **2004**, *429*, 52–55.
30. Ganeva, D.; Antonietti, M.; Faul, C. F. J.; Sanderson, R. D. Polymerization of the Organized Phases of Polyelectrolyte-Surfactant Complexes. *Langmuir* **2003**, *19*, 6561–6565.
31. Ganeva, D.; Faul, C. F. J.; Gotz, C.; Sanderson, R. D. Directed Reactions within Confined Reaction Environments: Polyadditions in Polyelectrolyte-Surfactant Complexes. *Macromolecules* **2003**, *36*, 2862–2866.
32. Mueller, A.; O'Brien, D. Supramolecular Materials *via* Polymerization of Mesophases of Hydrated Amphiphiles. *Chem. Rev.* **2002**, *102*, 727–758.
33. Summers, M.; Eastoe, J. Applications of Polymerizable Surfactants. *Adv. Colloid Interface Sci.* **2003**, *100−102*, 137–152.
34. Lee, Y.-S.; Yang, J.-Z.; Sisson, T. M.; Frankel, D. A.; Gleeson, J. T.; Aksay, E.; Keller, S. L.; Gruner, S. M.; O'Brien, D. Polymerization of Nonlamellar Lipid Assemblies. *J. Am. Chem. Soc.* **1995**, *117*, 5573–5578.
35. Dreja, M.; Lennartz, W. Polymerizable Polyelectrolyte-Surfactant Complexes from Monomeric Ammonium Cations and Polystyrenesulfonate. *Macromolecules* **1999**, *32*, 3528–3530.
36. Zimmerman, S. C.; Zeng, F. W.; Reichert, D. E. C.; Kolotuchin, S. V. Self-assembling Dendrimers. *Science* **1996**, *271*, 1095–1098.
37. Elmer, S. L.; Lemcoff, N. G.; Zimmerman, S. C. Exploring the Reversibility of the Ring-Closing Metathesis Mediated Cross-linking of Dendrimers. *Macromolecules* **2007**, *40*, 8114–8118.
38. Omastova, M.; Trchova, M.; Kovarova, J.; Stejskal, J. Synthesis and Structural Study of Polypyrroles Prepared in the Presence of Surfactants. *Synth. Met.* **2003**, *138*, 447–455.
39. Ikegame, M.; Tajima, K.; Aida, T. Template Synthesis of Polypyrrole Nanofibers Insulated within One-Dimensional Silicate Channels: Hexagonal versus Lamellar for Recombination of Polarons into Bipolarons. *Angew. Chem., Int. Ed.* **2003**, *42*, 2154–2157.
40. Li, G.; Bhosale, S.; Wang, T.; Zhang, Y.; Zhu, H.; Fuhrhop, J.-H. Gram-Scale Synthesis of Submicrometer-Long Polythiophene Wires in Mesoporous Silica Matrices. *Angew. Chem., Int. Ed.* **2003**, *42*, 3818–3821.
41. Spange, S. Insulated Nanowire Bundles through Consecutive Template Synthesis. *Angew. Chem., Int. Ed.* **2003**, *42*, 4430–4432.
42. Cao, Y.; Smith, P.; Heeger, A. J. Counterion Induced Processibility of Conducting Polyaniline and of Conducting Polyblends of Polyaniline in Bulk Polymers. *Synth. Met.* **1992**, *48*, 91–97.
43. Huang, J. X.; Virji, S.; Weiller, B. H.; Kaner, R. B. Polyaniline Nanofibers: Facile Synthesis and Chemical Sensors. *J. Am. Chem. Soc.* **2003**, *125*, 314–315.
44. Acik, M.; Sonmez, G. Nanofabrication of Aligned Conducting Polymers. *Polym. Adv. Technol.* **2006**, *17*, 697–699.

45. Taranekar, P.; Baba, A.; Fulghum, T.; Advincula, R. Conjugated Polymer Network Films from Precursor Polymers: Electrocopolymerization of a Binary Electroactive Monomer Composition. *Macromolecules* **2005**, *38*, 3679–3687.
46. Witker, D.; Reynolds, J. R. Soluble Variable Color Carbazole-Containing Electrochromic Polymers. *Macromolecules* **2005**, *38*, 7636–7644.
47. Gaupp, C. L.; Reynolds, J. R. Multichromic Copolymers Based on 3,6-Bis(2-(3,4-ethylenedioxythiophene))-*N*-alkylcarbazole Derivatives. *Macromolecules* **2003**, *36*, 6305–6315.
48. Sotzing, G. A.; Reddinger, J. L.; Katritzky, A. R.; Soloducho, J.; Musgrave, R.; Reynolds, J. R. Multiply Colored Electrochromic Carbazole-Based Polymers. *Chem. Mater.* **1997**, *9*, 1578–1587.
49. Reddinger, J. L.; Sotzing, G. A.; Reynolds, J. R. Multi-Colored Electrochromic Polymers Derived from Easily Oxidized Bis(2-(3,4-ethylenedioxy)thienyl) Carbazoles. *Chem. Commun.* **1996**, *15*, 1777–1778.
50. Baba, A.; Onishi, K.; Knoll, W.; Advincula, R. C. Investigating Work Function Tunable Hole-Injection/Transport Layers of Electrodeposited Polycarbazole Network Thin Films. *J. Phys. Chem. B* **2004**, *108*, 18949–18955.
51. Morin, J. F.; Leclerc, M. Synthesis of Conjugated Polymers Derived from *N*-Alkyl-2,7-carbazoles. *Macromolecules* **2001**, *34*, 4680–4682.
52. Zottii, G.; Schiavon, G.; Zecchin, S; Morin, J. F; Leclerc, M. Electrochemical, Conductive, and Magnetic Properties of 2,7-Carbazole-Based Conjugated Polymers. *Macromolecules* **2002**, *35*, 2122–2128.
53. Morin, J. F.; Leclerc, M. 2,7-Carbazole-Based Conjugated Polymers for Blue, Green, and Red Light Emission. *Macromolecules* **2002**, *35*, 8413–8417.
54. Morin, J. F.; Drolet, N.; Tao, Y.; Leclerc, M. Synthesis and Characterization of Electroactive and Photoactive 2,7-Carbazolenevinylene-Based Conjugated Oligomers and Polymers. *Chem. Mater.* **2004**, *16*, 4619–4626.
55. Morin, J. F.; Leclerc, M.; Ades, D.; Siove, A. Polycarbazoles: 25 Years of Progress. *Macromol. Rapid Commun.* **2005**, *26*, 761–778.
56. Taranekar, P.; Fulghum, T.; Patton, D.; Ponnapati, R.; Clyde, G.; Advincula, R. Investigating Carbazole Jacketed Precursor Dendrimers: Sonochemical Synthesis, Characterization, and Electrochemical Crosslinking Properties. *J. Am. Chem. Soc.* **2007**, *129*, 12537–12548.
57. Hartmann, P. C.; Dieudonne, P.; Sanderson, R. D. Self-assembly and Influence of the Organic Counterion in the Ternary Systems Dodecylamine/Acrylic Acid/Water and Dodecylamine/Methacrylic Acid/Water. *J. Colloid Interface Sci.* **2005**, *284*, 289–297.
58. Popova, M. V.; Tchernyshev, Y. S.; Michel, D. NMR Investigation of the Short-Chain Ionic Surfactant-Water Systems. *Langmuir* **2004**, *20*, 632–636.
59. Shimizu, S.; Pires, P. A. R.; El Seoud, O. A. ^{1}H and ^{13}C NMR Study on the Aggregation of (2-Acylaminoethyl)trimethylammonium Chloride Surfactants in D_2O. *Langmuir* **2003**, *19*, 9645–9652.
60. Fulghum, T.; Karim, S. M. A.; Baba, A.; Taranekar, P.; Nakai, T.; Masuda, T.; Advincula, R. C. Conjugated Poly(phenylacetylene) Films Cross-Linked with Electropolymerized Polycarbazole Precursors. *Macromolecules* **2006**, *39*, 1467–1473.
61. Taranekar, P.; Fulghum, T.; Baba, A.; Nakai, T.; Patton, D.; Advincula, R. C. Quantitative Electrochemical and Electrochromic Behavior of Terthiophene and Carbazole Containing Conjugated Polymer Network Film Precursors: EC-QCM and EC-SPR. *Langmuir* **2007**, *23*, 908–917.
62. Taranekar, P.; Fan, X.; Advincula, R. Distinct Surface Morphologies of Electropolymerized Polymethylsiloxane Network Polypyrrole and Comonomer Films. *Langmuir* **2002**, *18*, 7943–7952.
63. Inaoka, S.; Advincula, R. Synthesis and Oxidative Cross-Linking of Fluorene-Containing Polymers to Form Conjugated Network Polyfluorenes: Poly(fluoren-9,9-diyl-*alt*-alkan-,-diyl). *Macromolecules* **2002**, *35*, 2426–2428.
64. Hu, D. H.; Yu, J.; Barbara, P. F. Single-Molecule Spectroscopy of the Conjugated Polymer MEH-PPV. *J. Am. Chem. Soc.* **1999**, *121*, 6936–6937.
65. Sluch, M. I.; Godt, A.; Bunz, U. H. F.; Berg, M. A. Excited-State Dynamics of Oligo(p-phenyleneethynylene): Quadratic Coupling and Torsional Motions. *J. Am. Chem. Soc.* **2001**, *123*, 6447–6448.
66. Liu, M.; Kaur, P.; Waldeck, D. H.; Xue, C.; Liu, H. Fluorescence Quenching Mechanism of a Polyphenylene Polyelectrolyte with Other Macromolecules: Cytochrome c and Dendrimers. *Langmuir* **2005**, *21*, 1687–1690.
67. Thunemann, A. F.; Kubowicz, S.; Pietsch, U. Ultrathin Solid Polyelectrolyte-Surfactant Complex Films: Structure and Wetting. *Langmuir* **2000**, *16*, 8562–8567.
68. Thunemann, A. F.; Ruppelt, D.; Ito, S.; Mullen, K. Supramolecular Architecture of a Functionalized Hexabenzocoronene and Its Complex with Polyethyleneimine. *J. Mater. Chem.* **1999**, *9*, 1055–1057.
69. Ambrose, J. F.; Nelson, R. F. Anodic Oxidation Pathways of Carbazoles. 1. Carbazole and N-Substituted Derivatives. *J. Electrochem. Soc.* **1968**, *115*, 1159–1164.
70. Ambrose, J. F.; Carpenter, L. L.; Nelson, R. F. Electrochemical and Spectroscopic Properties of Cation Radicals. 3. Reaction Pathways of Carbazolium Radical Ions. *J. Electrochem. Soc.* **1975**, *122*, 876–894.
71. Mengoli, G.; Musiani, M. M.; Schreck, B. Electrochemical Synthesis and Properties of Polycarbazole Films in Protic Acid Media. *J. Electroanal. Chem.* **1988**, *246*, 73–76.
72. Cattarin, S.; Mengoli, G.; Musiani, M. M.; Schreck, B. Synthesis and Properties of Film Electrodes from N-Substituted Carbazoles in Acid Medium. *J. Electroanal. Chem.* **1988**, *246*, 87–100.
73. Huang, C.; Jiang, G.; Advincula, R. Electrochemical Crosslinking and Patterning of Nanostructured Polyelectrolyte Carbazole Precursor Ultrathin Films. *Macromolecules* **2008**, *41*, 4661.
74. Albertus, P. H.; Schenning, J.; Fransicus, B.; Benneker, G.; Hubertus, P.; Geurts, M.; Liu, X. Y.; Nolte, R. J. M. Porphyrin Wheels. *J. Am. Chem. Soc.* **1996**, *118*, 8549–8552.
75. Lee, E.; Jeong, Y. H.; Kim, J-K.; Lee, M. Controlled Self-Assembly of Asymmetric Dumbbell-Shaped Rod Amphiphiles: Transition from Toroids to Planar Nets. *Macromolecules* **2007**, *40*, 8355–8360.
76. Rakhmatullina, E.; Braun, T.; Chami, M.; Malinova, V.; Meier, W. Self-Organization Behavior of Methacrylate-Based Amphiphilic Di- and Triblock Copolymers. *Langmuir* **2007**, 12371–12379.
77. Suksai, C.; Gómez, S. F.; Chhabra, A.; Liu, J.; Skepper, J. N.; Tuntulani, T.; Otto, S. Controlling the Morphology of Aggregates of an Amphiphilic Synthetic Receptor through Host-Guest Interactions. *Langmuir* **2006**, *22*, 5994–5997.
78. Bo, Z. H.; Zhang, W. K.; Zhang, X.; Zhang, C. M.; Shen, J. C. Synthesis and Properties of Polyester Dendrimers Bearing Carbazole Groups in Their Periphery. *Macromol. Chem. Phys.* **1998**, *199*, 1323–1327.